

NEW IMAGING TECHNIQUE FOR MEASURING FLUID AND SOLID VELOCITIES IN SAND-LADEN FLOWS OVER DUNES IN AN OPEN CHANNEL

Kotaro CHICHIBU¹, Yasunori WATANABE² and Yasuyuki SHIMIZU³

¹ Dept. of Hydraulic Research, Hokkaido University

² Dr. Eng., Associate Professor, Dept. of Coastal & Offshore Engineering, Hokkaido University

³ Dr. Eng., Professor, Dept. of Hydraulic Research, Hokkaido University

Abstract

This paper presents quantitative energy and momentum exchanges between fluid and suspended sands via fluid-sand interactions in open channel flows over sandy dunes through comparisons of the sand-laden flow over movable bed and the single phase flows over the fixed bed, on the basis of double camera PIV measurements with an optical selection technique that is capable of measuring simultaneous velocities for the both water and sand phases at the same locations. Since a boundary shear layer formed behind the dunes is constrained to be developed over a movable bed, the turbulent energy on the separated shear layer is much lower than that in a fixed bed experiment. While the drag acting on the sands significantly decelerates the water flow above the shear layer at the inception of sand suspension, in a settling phase, the drag accelerates the water downward. Additional turbulent energy is induced during sand settlement process, which is over five times higher than the fixed bed case. This additional turbulence may disturb the bed surface and enhance re-suspension of the disturbed sands. This recursive energy and momentum exchanges between the sand and water flows via the suspension, diffusion, settlement and re-suspension processes have important roles to characterize the sand-laden flows over the movable sandy dunes.

Key Words : *dune, PIV, interaction, fixed bed, optical selection technique, turbulent energy*

1. INTRODUCTION

Turbulence induced in a shear layer near a river sand-bed disturbs a movable sand layer to pick up sands and carry them to downstream, typically resulting in a formation of sand-laden turbulent flows. The presence of suspended sands produces additional turbulence around them and often affects the carrying flows due to the sand-induced turbulence as well as drag force directory received from the carried sands. The energy exchange between fluid and solid particles, and also energy transfer from the carrying flow to turbulence may depend on relative length scales of turbulence and a particle (Gore and Crow, 1989). These effects induced by the suspended sands may appear to change the suspension process and deformation process of a local bed shape.

In an open channel flows with movable sandy dunes, initial sand suspensions change local flow field involving separations of a shear layer developing behind a dune crest. Since the sand suspension is also enhanced there due to high vertical shear within a separated vortex, details of fluid-solid interactions in turbulent flows involving separated vortices needs to be understood for estimating net flux of sediments. However, there has been few research on the dynamic interaction between water and suspended sands and its effect to water flow field since it was very difficult to experimentally measure local velocities of individual sand particles behind dunes.

Particle imaging velocimetry (PIV) has been commonly used for measuring spatial distributions of particle velocities, and many applications to open channel flows have been done (e.g. Anugrah et al, 2006). In this study, PIV was also employed for estimating simultaneous velocity distributions for both water and sand phases over a movable bed involving dunes on the basis of an optical selection technique. Effects of the presence of suspended sands to turbulence and mean flows were quantitatively estimated through comparisons with measurements for a single water phase over a fixed bed.

This paper organized as follows. In section 2, experimental set-up and our PIV technique are explained. The measurement results are discussed in section 3, and they are concluded in section 4.

2. EXPERIMENTS

(1) Experimental set-up

Experiments were conducted in an open channel of 10 m in length, 0.15 m in width and 0.3m in height with an uniform channel slope of 1:0.002 (see Fig. 1). Sands of which the mean diameter is 0.34 mm were used to form a sand layer of 50 mm thickness on a channel bottom. During experiments, the sands were consecutively supplied to maintain a constant layer thickness. Fluorescent neutral buoyant particles (diameter: 0.45 mm) were used as tracers of water flow. Movements of the tracers and suspended sands were recorded by two high-speed video cameras set in a dark room at the middle of the channel.

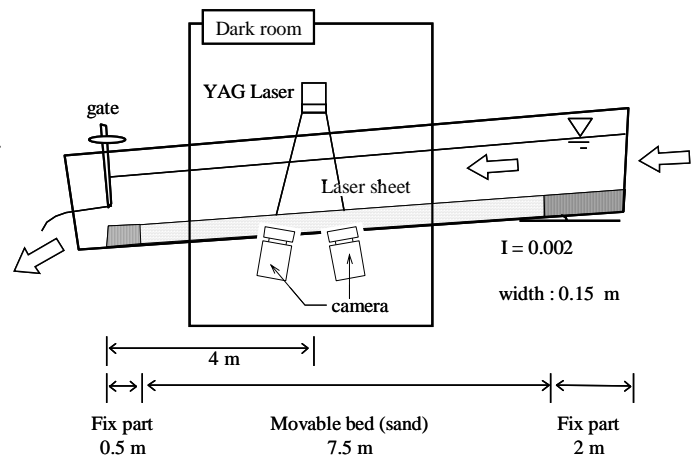


Fig. 1 Experimental set-up

Two cases of measurements were carried out for finding effects of the suspended sands over the movable sandy bed to turbulent and carrying mean flows. First, the simultaneous measurement of the tracers and sand particles over the movable bed (details of the measurement will be explained in the next subsection) was done (MB experiment). After this measurement, water in the channel was immediately drained, and the sand surface was covered with cement to create the fixed bed whose shape is identical with the previous sand bed. In the later experiment (FB experiment), only neutral buoyant tracers in an open-channel flow with the same discharge (6.84 l/s) as the former MB experiment were recorded at the same measurement location. The water depths for the former and later measurements were 112 mm and 104 mm, respectively. The formed dunes have roughly 17 mm of wave height and 240 mm of wavelength.

(2) Image acquisition and preprocessing

At the measurement location, a YAG laser (wavelength of 532 nm) sheet illuminated a stream-wise cross-section including the square field of view (FOV) of 100×100 mm over dunes. Two synchronized high-speed digital video cameras (resolution: 1 K \times 1 K pixels, frame rate: 500 fps) were mounted at one side of the channel to record the same FOV (see Fig. 2). The recorded images were sent to PC via an image

grabber connected with the cameras, and they were converted into 8-bit gray-scale bitmap.

In order to separately record each of the neutral buoyant tracer and suspended sand by different cameras, an optical selection technique was introduced. Since the laser beam is directory reflected on a surface of the sand particle, only the reflected lights from the sand can be recorded by one camera equipped an optical band-pass filter (band-pass: 527-537 nm). The fluorescent tracer used in the experiment is excited by the laser to emit fluorescent light of which the peak wavelength is about 570 nm. Therefore, using an optical high-pass filter (pass 550 nm or longer), the reflected light from the sands is prevented to be recorded, and only the fluorescent light from the tracers can be captured.

In a calibration procedure, a grid board was recorded by two cameras for obtaining calibration coefficients between image and real coordinates. The captured images were transformed to the real coordinates using linear projection based on the coefficients (see Fig. 3). Image noise was reduced by performing a Gaussian digital filter.

(3) PIV

PIV (Particle Image Velocimetry) is effective for measuring a plane distribution of local flow. In this study, the standard PIV algorithm (so-called cross-correlation method) was used. The cross-correlation of image intensities in interrogation area and search area for two consecutive frames is

$$R_{fg}(\Delta x, \Delta y) = \frac{\sum_{i=1}^N \sum_{j=1}^N [\{ f(x_i, y_j) - f_m \} \{ g(x_i + \Delta x, y_j + \Delta y) - g_m \}]}{\sqrt{\sum_{i=1}^N \sum_{j=1}^N \{ f(x_i, y_j) - f_m \}^2 \sum_{i=1}^N \sum_{j=1}^N \{ g(x_i + \Delta x, y_j + \Delta y) - g_m \}^2}} \quad (1)$$

where f and g are the image intensities in the interrogation and search areas, f_m and g_m are the mean image intensities over the both areas, respectively.

The window sizes of the interrogation and search areas were 55×55 pixels (5×5 mm) and 110×110 pixels (10×10 mm), respectively. An overlapping rate of the window was 50 %. The maximum correlation R_{max} was estimated at sub-pixel accuracy via second-order interpolation. For the window location where $R_{max} > 0.7$, the velocity is determined by

$$\mathbf{u} = \Delta \mathbf{x}_m / \Delta t \quad (2)$$

where \mathbf{x}_m is the displacement to give R_{max} . In cases that $R_{max} < 0.7$ and number of particles in the window are very small, the velocity is interpolated using the so-called square inverse distance method.

$$\mathbf{u}^* = \frac{\sum_{ij} \frac{\mathbf{u}_{ij}}{l_{ij}^2}}{\sum_{ij} \frac{1}{l_{ij}^2}} \quad (3)$$

where \mathbf{u}^* denotes the interpolated velocity, \mathbf{u}_{ij} is the reliable estimated velocity at distance l from the grid to be interpolated.

Accuracies of our PIV has been confirmed by using PIV standard images (PIV standardization and popularization project, visualization society of Japan); the relative standard deviation of the velocities was 4.97 % and correlation coefficient of the velocities was 0.97.

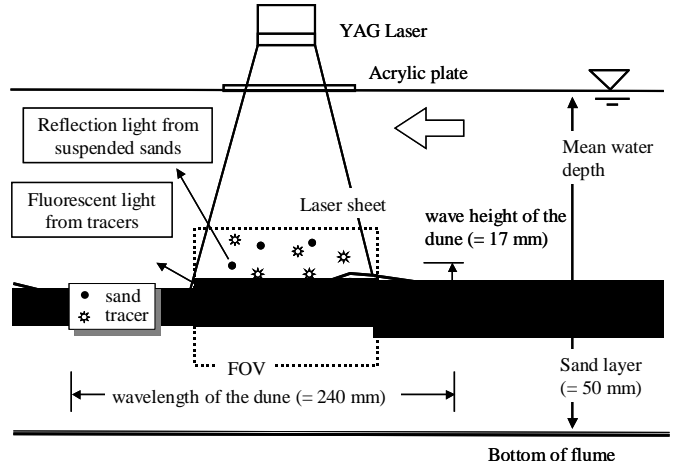


Fig. 2 Measurement location

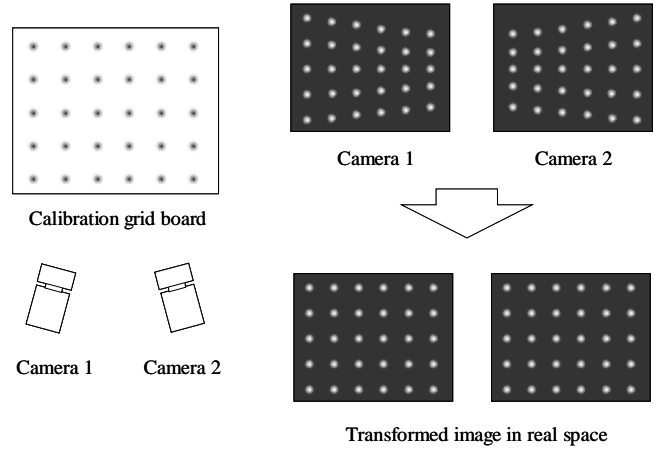


Fig. 3 Calibration procedure and image transformation.

(4) Turbulent statistics

Turbulence properties were statistically estimated on the basis of time-averaged velocity over 10 seconds (5000 video frames). It should be noted that 10 s is much longer than the time-scales of sand-induced turbulence and a primary vortex separated from the dune crest, and it is much shorter than the time-scale of propagation of the dunes. Therefore, it is an appropriate reference time-scale to be able to assume quasi-steady state.

The instantaneous velocity can be written as

$$\mathbf{u} = \overline{\mathbf{U}} + \mathbf{u}' \quad (4)$$

where \mathbf{U} is the time-averaged velocity and \mathbf{u}' is the fluctuation component. Subscript 'f' and 's' denotes fluid and sand. The turbulence energy can be defined by

$$k_f = \frac{1}{2}(\overline{u_f'^2} + \overline{v_f'^2}) \quad k_s = \frac{1}{2}(\overline{u_s'^2} + \overline{v_s'^2}) \quad (5)$$

and Reynolds stress is

$$\overline{u_f'v_f'}, \overline{u_s'v_s'} \quad (6)$$

The relative velocity between water and sand phases ($\mathbf{u}_r = \mathbf{u}_s - \mathbf{u}_f$) as a factor to determine drag force was also investigated.

$$\mathbf{u}_r = \overline{\mathbf{u}}_s - \overline{\mathbf{u}}_f \quad (7)$$

3. RESULT

(1) FIXED BED (FB) EXPERIMENT

Fig. 4 shows the velocity vector of the mean water flow passing over the fixed dune crest. A typical separation of a boundary shear layer appears just behind the crest, and the shear layer extends to downstream. A weak backward flow appears near the back slope of the dune, and a large-scale rotational flow is formed in a lower portion of the shear layer. High turbulent energy is found to be intensified along the separated shear layer since strong shear produces turbulence (see **Fig. 5**). The turbulent energy is also found to be diffused vertically.

There are high gradients of Reynolds stress near the separation point and also around the shear layer, suggesting vertical momentum transfers are significant in these regions (see **Fig. 6**).

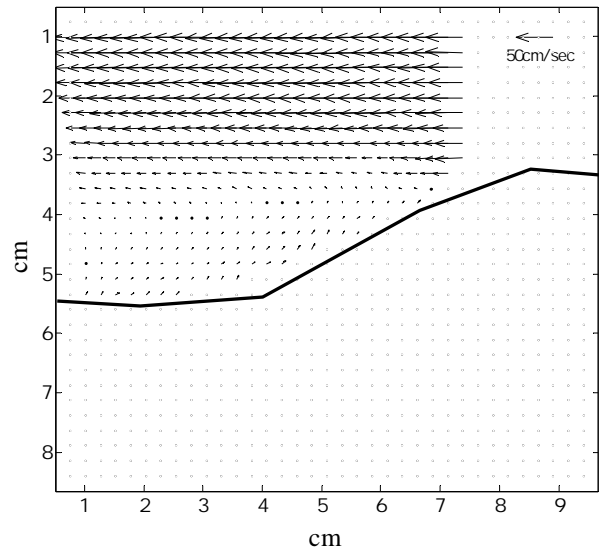


Fig. 4 Time-averaged velocities of water flow in FB case.

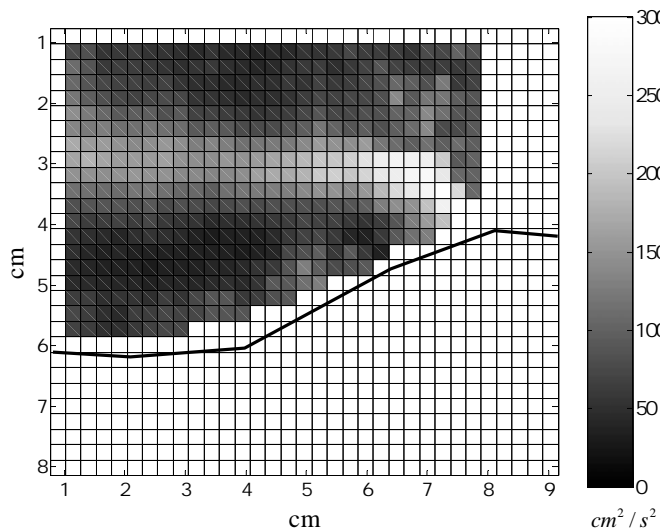


Fig. 5 Turbulence energy of water flow in FB case.

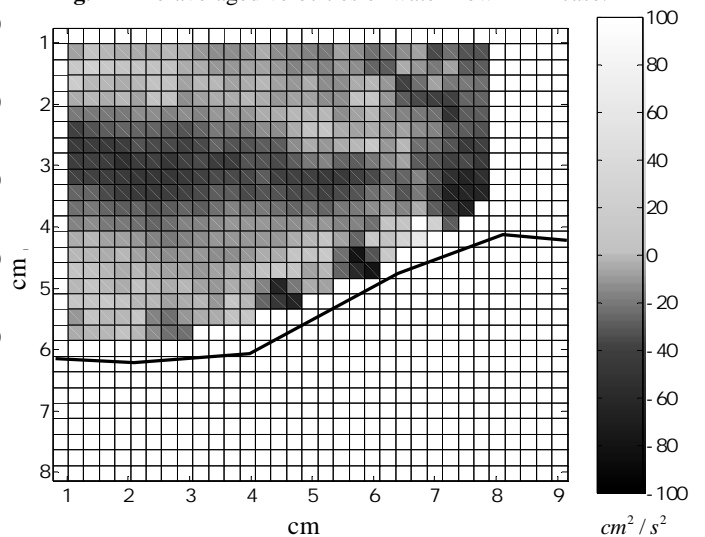


Fig. 6 Reynolds stress of water flow in FB case

(2) MOVABLE BED (MB) EXPERIMENT

While the shear boundary layer is significantly developed on a non-slip bottom surface where high velocity gradients occur in FB case, the velocity gradients near the movable bed are constrained to be mild since a thin upper layer of the sandy bed is drifted with the water flow (see **Fig. 7**). The resulting shear boundary layer is weak and the separation occurs at a lower portion of the back slope of the dune, resulting in weaker turbulent energy on the shear layer (see **Fig. 8**). On the other hand, the turbulent energy is found to be intensified and distributed in wide area of the downstream of the dune, which is a different feature with FB case in which no significant turbulent energy appears over the dune trough (see also **Fig. 5**). It has been confirmed that the settlement of the suspended sands is significant in this region, which suggests the intensified turbulence is due to additional turbulence produced during the settling process of suspended sands.

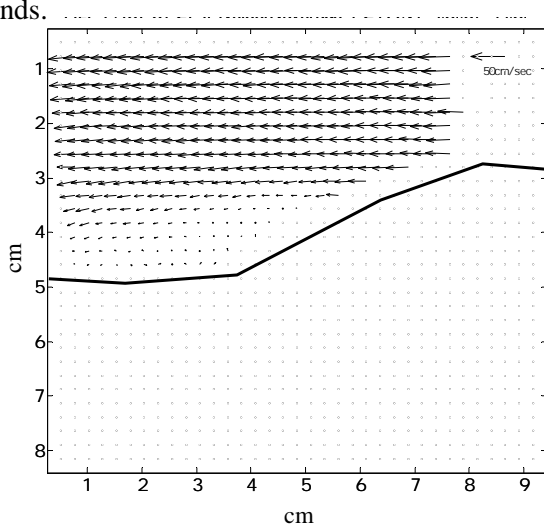


Fig. 8 Time-averaged velocities of water flow in MB case.

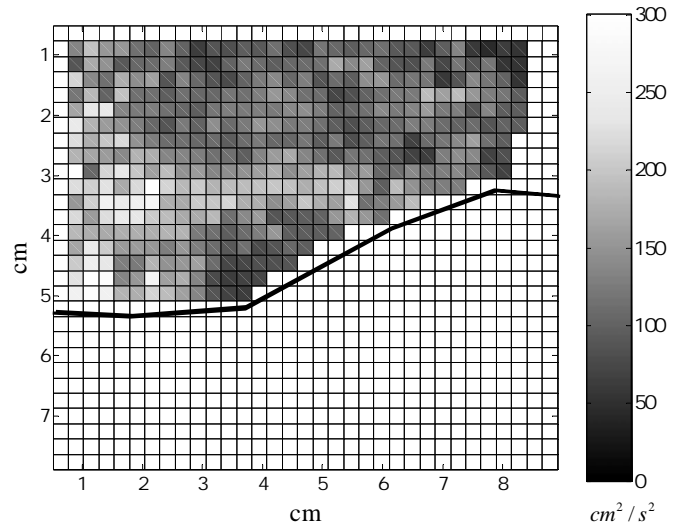


Fig. 7 Turbulent energy of water flow in MB case.

Dynamic contributions of the suspended sands to the carrying flow are discussed below. Since drag acting on a particle may be proportional to square of the relative velocity, the relative velocity ($u_r = u_s - u_f$) may be regarded as degree and direction to decelerate the water flow due to the drag of the suspended sands.

The high horizontal u_r occurs in the vicinity of the separation point while moderate u_r is also horizontally distributed above the separated shear layer (**Fig. 9**), which shows the suspended sands horizontally decelerate the water flow. In particular, high drag appearing at the separation point may be associated with the inception of sand suspension. The settling sands give downward drag to induce downward acceleration of the water flow beneath the shear layer.

Fig. 10 shows the difference in the water velocity ($u_{mov} - u_{fix}$) of FB and MB cases. It can be seen that, in MB case, the horizontal water velocity above the shear layer is lower and the velocity below the layer is higher than that in FB case. Despite the same water discharge with FB case was given to MB case, the maximum velocity of the carrying water flow decreases 5.5 % from that of FB case. This may be caused by the dynamic effects of the suspended sands to decelerate the water flow above the layer and to accelerate below the layer as already mentioned.

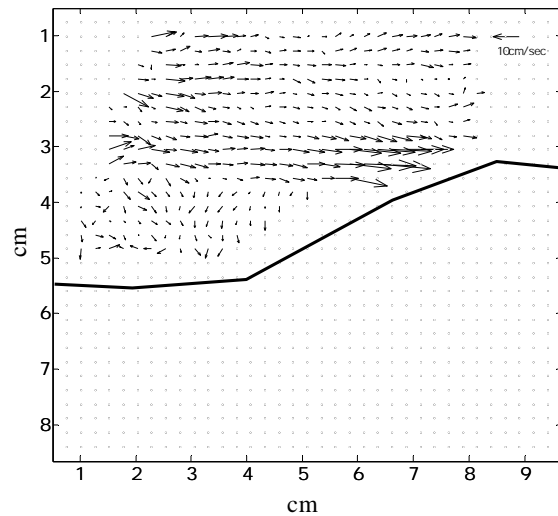


Fig. 9 Relative velocity of water and sand phases ($u_s - u_f$).

In the settling region, the turbulent energy in MB case is found to be significantly intensified over five times higher than that in FB case (see **Fig. 11**). This additional turbulence induced during the settling process may disturb the bed surface and enhance re-suspension of the disturbed sands.

This recursive energy and momentum exchanges between the sand and water flows via the suspension, diffusion, settlement and re-suspension processes have important roles to characterize the sand-laden flows over the movable sandy dunes.

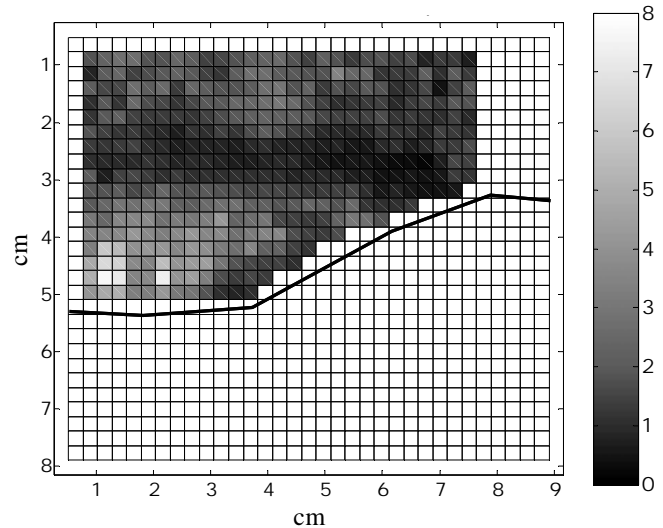
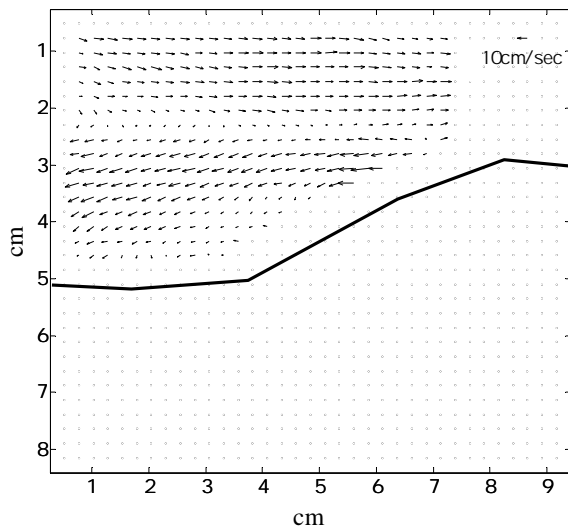


Fig. 10 Difference in the water velocities for FB and MB cases. **Fig. 11** Rate of turbulent energy between FB and MB case. (k_{MB}/k_{FD}).

4. CONCLUSIONS

In this paper, energy and momentum exchanges between fluid and suspended sands via fluid-sand interactions in open channel flows over sandy dunes is investigated through comparisons of the sand-laden flow over movable bed and the single phase flows over the fixed bed. Simultaneous velocities for the both water and sand phases at the same locations are successfully measured on the basis of double camera PIV system with an optical selection technique.

Since a boundary shear layer formed behind the dunes is constrained to be developed over a movable bed, the turbulent energy on the separated shear layer is much lower than that in no sand over a fixed bed experiment.

While the drag acting on the sands significantly decelerates the water flow above the shear layer at the inception of sand suspension, in a settling phase, the drag accelerate the water downward.

Additional turbulent energy is induced during sand settlement process, which is over five times higher than the fixed bed case. This additional turbulence may disturb the bed surface and enhance re-suspension of the disturbed sands.

It is found that this recursive energy and momentum exchanges between the sand and water flows via the suspension, diffusion, settlement and re-suspension processes have important roles to characterize the sand-laden flows over the movable sandy dunes.

REFERENCES

- 1) Gore, R. A. & Crowe, C. T. 1989. Effect of particle size on modulating turbulent intensity, *Int. J. Multiphase Flow*, Vol.15, pp.279-285.
- 2) Singh, A., Nir, A. & Semiat, R. 2006. Free-surface flow of concentrated suspensions, *Int. J. Multiphase Flow*, Vol.32, pp.775-790.
- 3) Visualization society of Japan. Standardization and popularization project. Standard images. (<http://www.vsj.or.jp/piv/>)